ANALYSIS OF THE SPECIFIC FORCE ON END MILLING

Anna Carla Araujo, José Luís Silveira

22nd IBERIAN LATIN-AMERICAN CONGRESS ON COMPUTATIONAL METHODS IN ENGINEERING
2nd Brazilian Congress on Computational Mechanics
NOVEMBER 7-9, 2001
Campinas, SP - Brazil

ANALYSIS OF THE SPECIFIC FORCE ON END MILLING

Anna Carla Araujo
José Luís Silveira
Programa de Engenharia Mecânica / COPPE / UFRJ - P.O. Box 68503 – 21945-970
Rio de Janeiro, RJ, Brazil.

Abstract. *An analysis of specific cutting pressure in end milling process is presented. To model analytically milling forces it is necessary to compute the chip volume and the specific cutting pressure. The problem is concerned on the exact geometrical formulation of the process and especially on the last parameter. Considering only the influence of shearing and friction on the rake face and not taking into consideration the effects on cutting of the flank face i.e. the edge effects, the results obtained shown an error proportional to the contribution of the tool contact with the finished surface. This work aims taking the value, or the variation, of specific pressure from experimental data considering both effects, cutting force and edge force. This procedure analyzes the influence of the specific force modelling on the cutting process.*

Keywords: *specific cutting force, end milling, machining modelling*

1. INTRODUCTION

In the end milling process there is a periodically varying chip cross section during the material removal and due to this the cutting force also varies. Accurate modelling of the cutting forces is required to predict the cutting forces, vibration, surface quality, and stability of machining processes.

A number of different methods to predict cutting forces have been developed over the last years. These models can be classified into three major categories: analytical, empirical, and mechanistic methods.

Analytical approaches, (Armarego & Brown, 1969), (Altintas, 2000), model the physical mechanisms that occur during cutting. This includes complex mechanisms such as high strain rates, high temperature gradients and combined elastic and plastic deformations and it's not yet completely solved. (Moufki et al, 2000)

In the empirical methods, a number of machining experiments are performed and performance measures such as cutting forces, tool life, and tool wear are measured (Armarego & Brown, 1969).

Mechanistic models, (Tlusty & MacNeil, 1975), (Kline, DeVor and Lindberg, 1982), (Altintas & Spence, 1991), (Yun & Cho, 2001) and (Jayaram, Kapoor and DeVor, 2001), predict the cutting forces based on a method that assumed cutting force to be proportional to the chip cross-sectional area.

The constants of proportionality are called the specific cutting pressures and depend on the cutter geometry, cutting conditions, insert grade and work piece material properties. This paper questions the behavior in time of specific cutting pressures for cutting force models for end milling process, estimating the specific cutting pressures directly from experimental cutting force data.

2. CUTTING FORCE MODELLING OF END MILLING OPERATIONS

Instantaneous differential cutting force for one single flute was written by Martelotti (Tlusty & MacNeil, 1975):

$$d\vec{F}_{cutting} = \vec{K}_{cutting}\, t\, db \tag{1}$$

where t is the uncut chip thickness and db is a differential piece of the depth of cut.

And was rewritten by (Armarego, 1989) adding the edge parcel:

$$\begin{aligned} d\vec{F} &= d\vec{F}_{edge} + d\vec{F}_{cutting} \\ d\vec{F} &= \vec{K}_{edge}\, db + \vec{K}_{cutting}\, t\, db \end{aligned} \tag{2}$$

where $\vec{K}_{edge}$ and $\vec{K}_{cutting}$ are vectors called specific edge force and specific cutting force, respectively.

The uncut chip thickness t for end milling is written as:

$$t = s_t \sin\phi \tag{3}$$

where ϕ is the angle of the cutting piece measured in relation of the normal direction of the feed per tooth s_t,

$$s_t = \frac{v}{\omega\ N_f} \tag{4}$$

from known v, ω and N_f as the feed velocity, rotation velocity and the number of flutes.

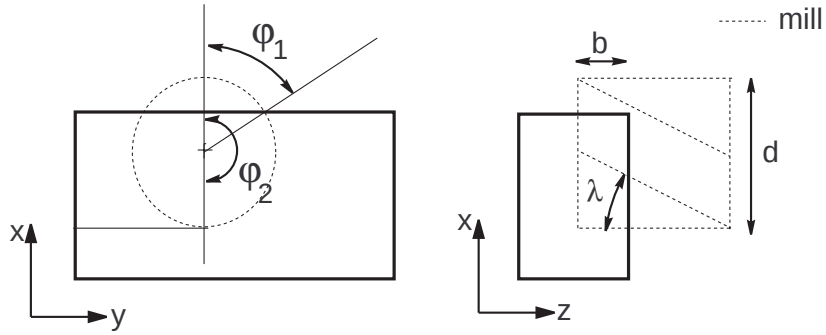

Figure 1: Milling geometry

The cutting tool pieces can be calculated by

$$db = \frac{d}{2\ \tan\lambda} d\phi \tag{5}$$

where d is the tool diameter and λ is the helix angle, as shown in Fig. 1.

The angle δ is calculated by

$$\delta = \frac{2\,b \tan\lambda}{d} \tag{6}$$

where b is the the depth of cut.

The angle δ is used to classify the cutting geometry as *Type I* or *Type II*,

$$\begin{array}{lll} \textit{Type I} & \longrightarrow & \delta \leq \varphi_2 - \varphi_1 \\ \textit{Type II} & \longrightarrow & \delta > \varphi_2 - \varphi_1 \end{array} \tag{7}$$

where φ_1 and φ_2 are the entry and exit angles, respectively (Fig. 1), enlightened on (Tlusty & MacNeil, 1975) and (Araujo & Silveira, 1999).

The force become:

$$\vec{F} = \int \vec{K}_{edge} db + \int \vec{K}_{cutting}\, t\, db = \int \left(\vec{K}_{edge} + \vec{K}_{cutting}\, s_t\, \sin\phi\right) \frac{d}{2\ \tan\lambda} d\phi \tag{8}$$

So, the total force of cut, considering the N_f flutes of the mill, are calculated by the sum:

$$\vec{F} = \sum_{i=1}^{N_f} \vec{F_i} \tag{9}$$

In this approach, all force contributions are calculated at the same time because all differential parts of the force are calculated for each cutting piece.

The time variation of the milling force vector ($\vec{\mathbf{F}}(t)$) is written as the multiplication of functions in time.

$$\vec{\mathbf{F}}(t) = \vec{\mathbf{K}}_{edge}(t)\mathbf{h}(t) + \vec{\mathbf{K}}_{cutting}(t)\mathbf{A}(t) \tag{10}$$

The specific forces, written as a vector function, ($\vec{\mathbf{K}}_{edge}(t)$ and $\vec{\mathbf{K}}_{cutting}(t)$), are multiplied by a scalar function relative to the height cutting ($\mathbf{h}(t)$) and other relative to the cutting area, the scalar function ($\mathbf{A}(t)$). This form is called from now on by *Functional approach*.

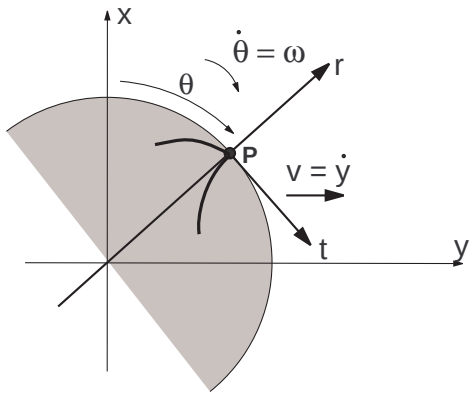

Figure 2: Milling Tool Referential

The time variable t can be substituted by the angle of rotation θ of a fixed point **P** in a peripheral tool and the tool velocity rotation ω as shown in Fig. 2.

$$\vec{\mathbf{F}}(t) = \tilde{\mathbf{F}}\left(\frac{\theta}{\omega}\right) = \vec{F}(\theta) \tag{11a}$$

$$\vec{F}(\theta) = \vec{K}_{edge}(\theta)h(\theta) + \vec{K}_{cutting}(\theta)A(\theta) \tag{11b}$$

The functions $h(\theta)$ and $A(\theta)$ will be calculated separately in the following sections.

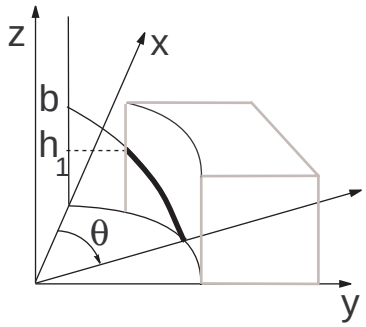

Figure 3: Height of cutting

Table 1: Integration limits for each phase.

	Type I		Type II	
Phase	$L_1(\theta)$	$L_2(\theta)$	$L_1(\theta)$	$L_2(\theta)$
For $e_1 < \theta \leq e_2$ - Phase A	φ_1	θ	φ_1	θ
For $e_2 < \theta \leq e_3$ - Phase B	$\theta - \delta$	θ	φ_1	φ_2
For $e_3 < \theta \leq e_4$ - Phase C	$\theta - \delta$	φ_2	$\theta - \delta$	φ_2

3. THE HEIGHT FUNCTION

In Fig. 3. can be observed the height of cutting of the first flute (h_1) at the milling angle θ, for a cutting geometry.

The height function of cutting of the first flute $h_1(\theta)$ can be calculated by:

$$h_1(\theta) = \int_{L_1(\theta)}^{L_2(\theta)} \frac{d}{2\ \sin\lambda}\, d\varepsilon \tag{12}$$

where the limits L_1 and L_2 are functions of θ and are calculated differently for each cutting phase of θ as can be observed on Table 1 and the values of e_1, e_2, e_3 and e_4 can be extracted from Table 2.

In order to add the contributions of all flutes, the height of cutting for any flute (*n*) is written by:

$$h_n(\theta) = \int_{L_1(\theta+\xi(n-1))}^{L_2(\theta+\xi(n-1))} \frac{d}{2\ \sin\lambda}\, d\varepsilon \tag{13}$$

Note that the functions L_1 and L_2 are now not only a function of θ but also a function of n, where ξ is the angle between the flutes.

Table 2: Variables values

	Type I	Type II
e_1	φ_1	φ_1
e_2	$\varphi_1 + \delta$	φ_2
e_3	φ_2	$\varphi_1 + \delta$
e_4	$\varphi_2 + \delta$	$\varphi_2 + \delta$

The total length is calculated by:

$$h(\theta) = \sum_{n=1}^{N_f} h_n(\theta) \tag{14}$$

A height function of each flute, for a four flute tool, is presented in Fig. 4.

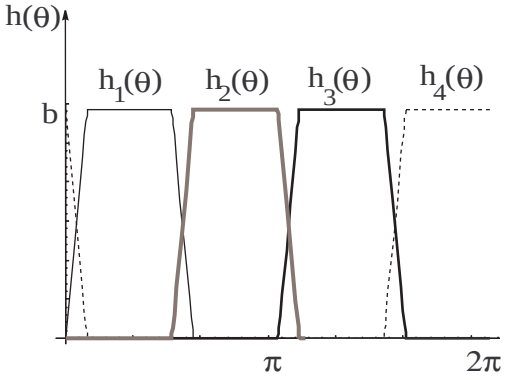

Figure 4: Function of height of cutting

4. THE CROSS-SECTIONAL AREA VARIATION

In Fig. 5 can be observed the chip cross-sectional area (A_1) of the first flute at milling angle θ, for a cutting geometry having $\varphi_1 = 30^o$ and $\varphi_2 = \pi/2$.

The chip area can be calculated by:

$$A_1(\theta) = \int_{L_1(\theta)}^{L_2(\theta)} \frac{s_t\, d}{2\, \sin\lambda} \sin\phi\, d\phi \tag{15}$$

where the limits L_1 and L_2 are functions of θ and are calculated differently for each cutting phase of θ as can be observed on Table 1.

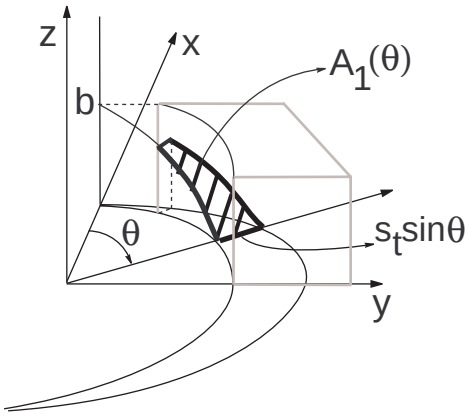

Figure 5: Chip Cross-sectional Area

For a single flute and *Type I* cutting geometry, the chip cross-sectional area function is presented on Fig. 6. In order to add the contributions of all flutes, the chip cross-sectional area function for any flute (*n*) is written by:

$$A_n(\theta) = \int_{L_1(\theta+\xi(n-1))}^{L_2(\theta+\xi(n-1))} \frac{s_t\, d}{2\, \sin\lambda} \sin\varepsilon\, d\varepsilon \tag{16}$$

Note that the functions L_1 and L_2 are now not only a function of θ but also a function of n, where ξ is the angle between the flutes.

The total area is calculated by:

$$A(\theta) = \sum_{n=1}^{N_f} A_n(\theta) \tag{17}$$

and the figure 7 shows the chip cross-sectional area function $A(\theta)$ for a milling with four flutes ($\xi = 90^o$) and in bold the function of the first flute $A_1(\theta)$, of a cut having *Type I* geometry.

5. FORCE COMPUTATION

In order to compare the present model with experimental data, the force components should be decomposed in x, y and z directions as they are usually recorded in machining tests.

$$\vec{F}(\theta) = \begin{bmatrix} F_x(\theta) \\ F_y(\theta) \\ F_z(\theta) \end{bmatrix} = A(\theta) \begin{bmatrix} K_{cx}(\theta) \\ K_{cy}(\theta) \\ K_{cz}(\theta) \end{bmatrix} + h(\theta) \begin{bmatrix} K_{ex}(\theta) \\ K_{ey}(\theta) \\ K_{ez}(\theta) \end{bmatrix} \tag{18}$$

But it's not convenient to write the specific cutting force in the fixed referential x, y, z. To rewrite it on the more appropriate tool referential t, r, z (tangential, radial and axial directions),

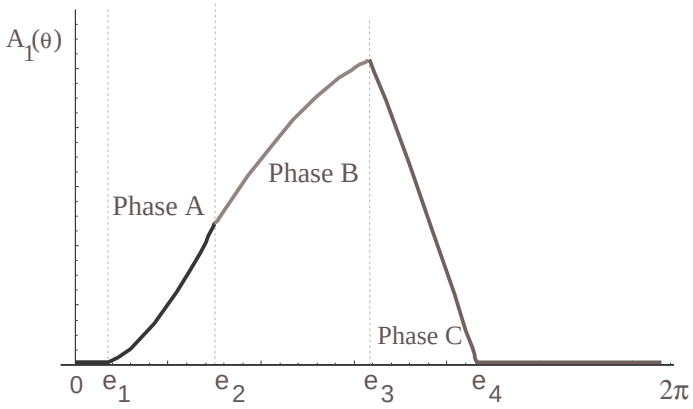

Figure 6: Area Function for one Single Flute

another functions $A_R(\theta)$ and $h_R(\theta)$ has to be introduced:

$$\begin{bmatrix} F_x(\theta) \\ F_y(\theta) \\ F_z(\theta) \end{bmatrix} = A_R(\theta) \begin{bmatrix} K_{ct}(\theta) \\ K_{cr}(\theta) \\ K_{cz}(\theta) \end{bmatrix} + h_R(\theta) \begin{bmatrix} K_{et}(\theta) \\ K_{er}(\theta) \\ K_{ez}(\theta) \end{bmatrix} \tag{19}$$

In fact, the function $A_R(\theta)$ and $h_R(\theta)$ are the rotation matrix $\mathbf{R}(\theta)$ multiplied by the area and the height, respectively.

$$\mathbf{R}(\theta) = \begin{pmatrix} \cos(\theta) & \sin(\theta) & 0 \\ \sin(\theta) & -\cos(\theta) & 0 \\ 0 & 0 & 1 \end{pmatrix} \tag{20}$$

The rotation matrix $\mathbf{R_n}(\theta)$ have to be written for each flute:

$$\mathbf{R_n}(\theta) = \begin{pmatrix} \cos(\theta + \xi\,(n-1)) & \sin(\theta + \xi\,(n-1)) & 0 \\ \sin(\theta + \xi\,(n-1)) & -\cos(\theta + \xi\,(n-1)) & 0 \\ 0 & 0 & 1 \end{pmatrix} \tag{21}$$

Then, for all flutes, the rotated area function becomes:

$$A_R(\theta) = \sum_{n=1}^{N_f} \mathbf{R_n}(\theta)\, A_n(\theta) \tag{22}$$

and the rotated length function is:

$$h_R(\theta) = \sum_{n=1}^{N_f} \mathbf{R_n}(\theta)\, h_n(\theta) \tag{23}$$

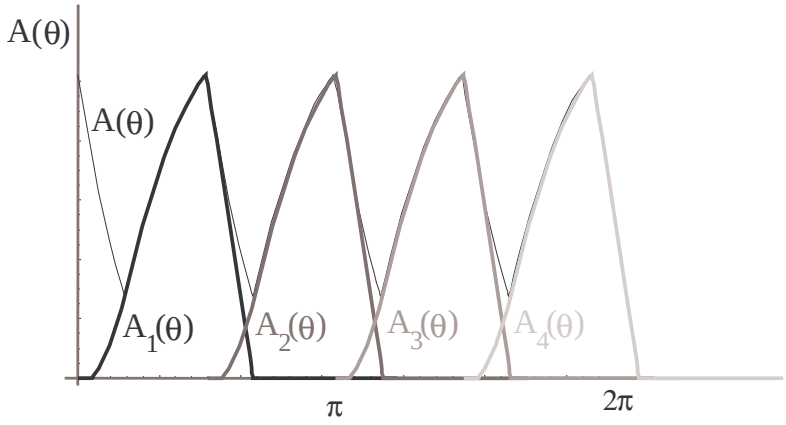

Figure 7: End Milling Area Function

To simplify the following calculations, $S_1(\theta)$, $S_2(\theta)$, $S_3(\theta)$ and $S_4(\theta)$are defined:

$$S_1(\theta) = \sum_{n=1}^{N_f} A_n(\theta)\ \cos(\theta + \xi\ (n-1)) \tag{24a}$$

$$S_2(\theta) = \sum_{n=1}^{N_f} A_n(\theta)\ \sin(\theta + \xi\ (n-1)) \tag{24b}$$

$$S_3(\theta) = \sum_{n=1}^{N_f} h_n(\theta)\ \cos(\theta + \xi\ (n-1)) \tag{24c}$$

$$S_4(\theta) = \sum_{n=1}^{N_f} h_n(\theta)\ \sin(\theta + \xi\ (n-1)) \tag{24d}$$

Rewriting the Eq. (19), the force can be expressed by:

$$\begin{bmatrix} F_x(\theta) \\ F_y(\theta) \\ F_z(\theta) \end{bmatrix} = A_R(\theta) \begin{bmatrix} K_{ct}(\theta) \\ K_{cr}(\theta) \\ K_{cz}(\theta) \end{bmatrix} + h_R(\theta) \begin{bmatrix} K_{et}(\theta) \\ K_{er}(\theta) \\ K_{ez}(\theta) \end{bmatrix} \tag{25a}$$

$$\begin{bmatrix} F_x(\theta) \\ F_y(\theta) \\ F_z(\theta) \end{bmatrix} = \begin{bmatrix} S_1(\theta) & S_2(\theta) & 0 & S_3(\theta) & S_4(\theta) & 0 \\ S_2(\theta) & -S_1(\theta) & 0 & S_4(\theta) & -S_3(\theta) & 0 \\ 0 & 0 & A(\theta) & 0 & 0 & h(\theta) \end{bmatrix} \begin{bmatrix} K_{ct}(\theta) \\ K_{cr}(\theta) \\ K_{cz}(\theta) \\ K_{et}(\theta) \\ K_{er}(\theta) \\ K_{ez}(\theta) \end{bmatrix} \tag{25b}$$

Note that the matrix $J(\theta)$ is the Jacobian of the $\mathbf{F}$ components in relation to the specific cutting force coefficients.

$$
\begin{aligned}
J(\theta) &= \begin{bmatrix} S_1(\theta) & S_2(\theta) & 0 & S_3(\theta) & S_4(\theta) & 0 \\ S_2(\theta) & -S_1(\theta) & 0 & S_4(\theta) & -S_4(\theta) & 0 \\ 0 & 0 & A(\theta) & 0 & 0 & h(\theta) \end{bmatrix} \\
&= \begin{bmatrix} \frac{\partial F_x}{\partial K_{ct}} & \frac{\partial F_x}{\partial K_{cr}} & \frac{\partial F_x}{\partial K_{cz}} & \frac{\partial F_x}{\partial K_{et}} & \frac{\partial F_x}{\partial K_{er}} & \frac{\partial F_x}{\partial K_{ez}} \\ \frac{\partial F_y}{\partial K_{ct}} & \frac{\partial F_y}{\partial K_{cr}} & \frac{\partial F_y}{\partial K_{cz}} & \frac{\partial F_y}{\partial K_{et}} & \frac{\partial F_y}{\partial K_{er}} & \frac{\partial F_y}{\partial K_{ez}} \\ \frac{\partial F_z}{\partial K_{ct}} & \frac{\partial F_z}{\partial K_{cr}} & \frac{\partial F_z}{\partial K_{cz}} & \frac{\partial F_z}{\partial K_{et}} & \frac{\partial F_z}{\partial K_{er}} & \frac{\partial F_z}{\partial K_{ez}} \end{bmatrix}
\end{aligned}
\tag{26}
$$

6. SPECIFIC FORCE ANALYSIS

The problem is concentrated on the specific force analysis. The Eq. (25) can be easily calculated if the specific pressures are constant in θ.

Empirical works, (Tlusty & MacNeil, 1975) and (Ber, Rotberg and Zombach, 1988), considered the specific force as one single value for each pair of tool-workpiece and relate the components by coefficients of proportionality; these researchers considers that the specific force is time constant.

Analytical approaches (Altintas, 2000) calculate the specific cutting forces as a function of cutting parameters.

Orthogonal and Oblique are the most well known models and these specific cutting forces are shown on Table 3, where ϕ is the shear angle, α the rake angle, β the friction angle, η the chip flow angle, and the lower index n means the normal component of the angles.

If these parameters are time constant, the specific cutting force do not change in time. To analyze this behavior, for each point of θ, the equation:

$$\mathbf{K}(\theta) = \mathbf{J^{-1}}(\theta)\mathbf{F}(\theta) \tag{27}$$

can be applied to any experimental data from milling process, then if the specific cutting force is constant, the result must has the same value.

The graphic from Fig. 8 was taken from (Altintas & Lee, 1996). This experiment used the following parameters:

$$d = 18.1mm, \quad \lambda = 30.0, \quad N_f = 4, \quad b = 5.08, \quad \varphi_1 = 0, \quad \varphi_2 = \frac{\pi}{2}, \quad v = 30\frac{m}{min}, \quad s_t = 0.05.$$

But, when calculating the Eq. 27, appears a singularity because there are three parameters

Table 3: Analytical Specific Force

	Orthogonal Model	Oblique Model
K_t	$\frac{\tau_s \cos(\beta-\alpha)}{\sin\phi\cos(\phi+\beta-\alpha)}$	$\frac{\tau_s}{\sin\phi_n}\frac{(\cos(\beta_n-\alpha_n)+\tan\lambda\ \tan\eta\ \sin\beta_n)}{\sqrt{\cos^2(\phi_n+\beta_n-\alpha_n)+\tan^2\eta\sin^2\beta_n}}$
K_r	$\frac{\tau_s \sin(\beta-\alpha)}{\sin\phi\cos(\phi+\beta-\alpha)}$	$\frac{\tau_s}{\sin\phi_n}\frac{(\cos(\beta_n-\alpha_n)\tan\lambda-\tan\eta\sin\beta_n)}{\sqrt{\cos^2(\phi_n+\beta_n-\alpha_n)+\tan^2\eta\sin^2\beta_n}}$
K_z	0	$\frac{\tau_s}{\sin\phi_n\cos\lambda}\frac{(\sin(\beta_n-\alpha_n))}{\sqrt{\cos^2(\phi_n+\beta_n-\alpha_n)+\tan^2\eta\sin^2\beta_n}}$

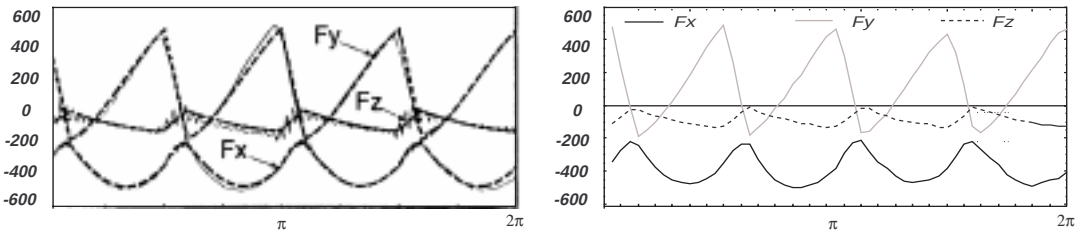

(a) Scan (b) Digital

Figure 8: Experimental data from (Altintas & Lee, 1996)

and six unknown variables.

$$\begin{bmatrix} F_x(\theta) \\ F_y(\theta) \\ F_z(\theta) \end{bmatrix} = \begin{bmatrix} S_1(\theta) & S_2(\theta) & 0 & S_3(\theta) & S_4(\theta) & 0 \\ S_2(\theta) & -S_1(\theta) & 0 & S_4(\theta) & -S_3(\theta) & 0 \\ 0 & 0 & A(\theta) & 0 & 0 & h(\theta) \end{bmatrix} \begin{bmatrix} K_{ct}(\theta) \\ K_{cr}(\theta) \\ K_{cz}(\theta) \\ K_{et}(\theta) \\ K_{er}(\theta) \\ K_{ez}(\theta) \end{bmatrix} \tag{28}$$

To solve this problem, we suppose that two consecutive points have the same specific force,

calculating the specific force for each interval:

$$\begin{bmatrix} F_x(\theta) \\ F_y(\theta) \\ F_z(\theta) \\ F_x(\theta+d\theta) \\ F_y(\theta+d\theta) \\ F_z(\theta+d\theta) \end{bmatrix} = J_A(\theta) \begin{bmatrix} K_{ct}(\theta) \\ K_{cr}(\theta) \\ K_{cz}(\theta) \\ K_{et}(\theta) \\ K_{er}(\theta) \\ K_{ez}(\theta) \end{bmatrix} \tag{29}$$

The matrix J amplified became a square matrix J_A:

$$J_A(\theta) = \begin{bmatrix} S_1(\theta) & S_2(\theta) & 0 & S_3(\theta) & S_4(\theta) & 0 \\ S_2(\theta) & -S_1(\theta) & 0 & S_4(\theta) & -S_3(\theta) & 0 \\ 0 & 0 & A(\theta) & 0 & 0 & h(\theta) \\ S_1(\theta+d\theta) & S_2(\theta+d\theta) & 0 & S_3(\theta+d\theta) & S_4(\theta+d\theta) & 0 \\ S_2(\theta+d\theta) & -S_1(\theta+d\theta) & 0 & S_4(\theta+d\theta) & -S_3(\theta+d\theta) & 0 \\ 0 & 0 & A(\theta+d\theta) & 0 & 0 & h(\theta+d\theta) \end{bmatrix} \tag{30}$$

and the problem has only one solution:

$$\begin{bmatrix} K_{ct}(\theta) \\ K_{cr}(\theta) \\ K_{cz}(\theta) \\ K_{et}(\theta) \\ K_{er}(\theta) \\ K_{ez}(\theta) \end{bmatrix} = [J_A(\theta)]^{-1} \begin{bmatrix} F_x(\theta) \\ F_y(\theta) \\ F_z(\theta) \\ F_x(\theta+d\theta) \\ F_y(\theta+d\theta) \\ F_z(\theta+d\theta) \end{bmatrix} \tag{31}$$

The Fig. 9 shows the result for specific pressures using the data from Fig. 8. Figures 9**a**, 9**b** and 9**c**, respectively tangential, radial and vertical specific cutting forces and 9**g**, 9**h** and 9**i**, are tangential, radial and vertical specific edge forces). Figures 9**d**, 9**e**, 9**f**, 9**j**, 9**k** and 9**l** are them distributions.

Calculating the average value of the specific values obtained for the hole rotation $\overline{K}$, and applying on Eq. 25 results:

$$\begin{bmatrix} F_x(\theta) \\ F_y(\theta) \\ F_z(\theta) \end{bmatrix} = J(\theta) \begin{bmatrix} \overline{K}_{ct} \\ \overline{K}_{cr} \\ \overline{K}_{cz} \\ \overline{K}_{et} \\ \overline{K}_{er} \\ \overline{K}_{ez} \end{bmatrix} \tag{32}$$

as shown in Table 4.

Table 4: Average Specific Pressure Values - N/mm^2

$\overline{K}_{ct}$	$\overline{K}_{cr}$	$\overline{K}_{cz}$	$\overline{K}_{et}$	$\overline{K}_{er}$	$\overline{K}_{ez}$
1150.5	341.0	436.7	24.1	42.2	0.4

Using these values to recalculate the forces, Fig. 10 shows the comparison between experimental force and semi-empirical force. This procedure aims to confirm if the behavior of the specific pressure considered is correct.

A general code of an end milling process is given on Table 5. The input variables set by the user are cutter radius, helix angle, entry and exit angles, axial depth of cut, the number of teeth, feed per tooth and the experimental cutting force.

Table 5: Algorithm to specific force analysis

1 Input experimental cutting force (Np points)

$$Fx_{exp}(j),\quad Fy_{exp}(j),\quad Fz_{exp}(j). \qquad j \in [1, Np]$$

2 Inputs: r, λ, N_n, b, φ_1, φ_2, v, s_t

3 Compute δ and ζ

4 Check for *Type I* or *Type II*

5 Compute e_1, e_2, e_3 and e_4

6 Compute $A(\theta) =$

$$\begin{cases} 0 & 0 \le \theta < e_1 \\ \int_{e_1}^{\theta} \frac{r}{\sin\lambda}\, s_t\, \sin\phi\, d\phi & e_1 \le \theta < e_2 \\ \int_{\theta-\delta}^{\theta} \frac{r}{\sin\lambda}\, s_t\, \sin\phi\, d\phi & e_2 \le \theta < e_3 \\ \int_{\theta-\delta}^{e_3} \frac{r}{\sin\lambda}\, s_t\, \sin\phi\, d\phi & e_3 \le \theta < e_4 \\ 0 & e_4 \le \theta < 2\pi \end{cases} \quad \text{if } \textit{Type I}$$

or $A(\theta) =$

$$\begin{cases} 0 & 0 \le \theta < e_1 \\ \int_{e_1}^{\theta} \frac{r}{\sin\lambda}\, s_t\, \sin\phi\, d\phi & e_1 \le \theta < e_2 \\ \int_{e_1}^{e_2} \frac{r}{\sin\lambda}\, s_t\, \sin\phi\, d\phi & e_2 \le \theta < e_3 \\ \int_{\theta-\delta}^{e_2} \frac{r}{\sin\lambda}\, s_t\, \sin\phi\, d\phi & e_3 \le \theta < e_4 \\ 0 & e_4 \le \theta < 2\pi \end{cases} \quad \text{if } \textit{Type II}$$

7 Compute $h(\theta) =$

$$\begin{cases} 0 & 0 \le \theta < e_1 \\ \int_{e_1}^{\theta} \frac{r}{\sin\lambda}\, d\phi & e_1 \le \theta < e_2 \\ \int_{\theta-\delta}^{\theta} \frac{r}{\sin\lambda}\, d\phi & e_2 \le \theta < e_3 \\ \int_{\theta-\delta}^{e_3} \frac{r}{\sin\lambda}\, d\phi & e_3 \le \theta < e_4 \\ 0 & e_4 \le \theta < 2\pi \end{cases} \quad \text{if } \textit{Type I}$$

or $h(\theta) =$

$$\begin{cases} 0 & 0 \le \theta < e_1 \\ \int_{e_1}^{\theta} \frac{r}{\sin\lambda}\, d\phi & e_1 \le \theta < e_2 \\ \int_{e_1}^{e_2} \frac{r}{\sin\lambda}\, d\phi & e_2 \le \theta < e_3 \\ \int_{\theta-\delta}^{e_2} \frac{r}{\sin\lambda}\, d\phi & e_3 \le \theta < e_4 \\ 0 & e_4 \le \theta < 2\pi \end{cases} \quad \text{if } \textit{Type II}$$

8 Compute

$$S_1(\theta) = \sum_{n=1}^{N_f} A(\theta + \xi(n-1))\, \cos(\theta + \xi(n-1))$$
$$S_2(\theta) = \sum_{n=1}^{N_f} A(\theta + \xi(n-1))\, \sin(\theta + \xi(n-1))$$
$$A_t(\theta) = \sum_{n=1}^{N_f} A(\theta + \xi(n-1))$$

$$S_3(\theta) = \sum_{n=1}^{N_f} h(\theta + \xi(n-1))\ \cos(\theta + \xi(n-1))$$
$$S_4(\theta) = \sum_{n=1}^{N_f} h(\theta + \xi(n-1))\ \sin(\theta + \xi(n-1))$$
$$h_t(\theta) = \sum_{n=1}^{N_f} h(\theta + \xi(n-1))$$

9 Discretize all functions

$$Sd_1(j) = S_1(\theta = \tfrac{2\pi\,(j-1)}{Np-1})$$

10 Compute $J_A(j)$

$$J_A(j) = \begin{bmatrix} Sd_1(j) & Sd_2(j) & 0 & Sd_3(j) & Sd_4(j) & 0 \\ Sd_2(j) & -Sd_1(j) & 0 & Sd_4(j) & -Sd_3(j) & 0 \\ 0 & 0 & Ad_t(j) & 0 & 0 & hd_t(j) \\ Sd_1(j+1) & Sd_2(j+1) & 0 & Sd_3(j+1) & Sd_4(j+1) & 0 \\ Sd_2(j+1) & -Sd_1(j+1) & 0 & Sd_4(j+1) & -Sd_3(j+1) & 0 \\ 0 & 0 & Ad_t(j+1) & 0 & 0 & hd_t(j+1) \end{bmatrix}$$

11 Compute the matrix $KG(j)$ with all specific pressures

$$KG(j) \;=\; J_A(j)^{-1} \,.\, \begin{bmatrix} Fx_{exp}(j) \\ Fx_{exp}(j) \\ Fx_{exp}(j) \\ Fx_{exp}(j+1) \\ Fx_{exp}(j+1) \\ Fx_{exp}(j+1) \end{bmatrix}$$

12 Compute each specific pressure

$$K_{ct}(j) = KG(j)_1$$
$$K_{cr}(j) = KG(j)_2$$
$$K_{cz}(j) = KG(j)_3$$
$$K_{et}(j) = KG(j)_4$$
$$K_{er}(j) = KG(j)_5$$
$$K_{ez}(j) = KG(j)_6$$

13 Compute average specific pressures

$$\overline{K_{ct}} = \sum_{j=1}^{Np} K_{ct}(j)$$
$$\overline{K_{cr}} = \sum_{j=1}^{Np} K_{cr}(j)$$
$$\overline{K_{cz}} = \sum_{j=1}^{Np} K_{cz}(j)$$
$$\overline{K_{et}} = \sum_{j=1}^{Np} K_{et}(j)$$
$$\overline{K_{er}} = \sum_{j=1}^{Np} K_{er}(j)$$
$$\overline{K_{ez}} = \sum_{j=1}^{Np} K_{ez}(j)$$

14 Use this values to calculate semi-empirical force

$$F_x(j) = \overline{K_{ct}} Sd_1(j) + \overline{K_{cr}} Sd_2(j) + \overline{K_{et}} Sd_3(j) + \overline{K_{er}} Sd_4(j)$$
$$F_y(j) = \overline{K_{ct}} Sd_2(j) - \overline{K_{cr}} Sd_1(j) + \overline{K_{et}} Sd_4(j) - \overline{K_{er}} Sd_3(j)$$
$$F_z(j) = \overline{K_{ct}} Sd_1(j) + \overline{K_{cr}} Sd_2(j) + \overline{K_{cz}} Ad_t(j) + \overline{K_{ez}} hd_t(j)$$

7. CONCLUSIONS

This paper analyzes the behavior of the specific cutting pressures from experimental cutting force data. A procedure to estimate the specific cutting forces from data is developed using the function approach including the edge parcel in the model. The method is validated by recalculation of the cutting force and compared with the experiment published by (Altintas & Lee, 1996). The contribution of the edge force is important to the model but there is no visual variation on time for them. The difference from results with and without the edge forces can be observed comparing with (Araujo & Silveira, 2001).

Acknowledgements

This research was partially supported by FUJB (Fundação Universitária José Bonifácio) under project 8451-4.

REFERENCES

Altintas, U., 2000, “Manufacturing Automation”, Cambridge University Press, 1st edition.

Altintas, U. & Lee, P., 1996, “A General Mechanics and Dynamics Model for Helical End Mills”, Annals of CIRP, Vol.45/1, pp. 59-64.

Altintas, U. & Spence, A., 1991,“End Milling force algorithm for CAD Systems”, Annals of CIRP, Vol.40/1, pp. 31-34.

Araujo, A.C. & Silveira,J.L., 1999,“Models for the Prediction of Instantaneous Cutting Forces in End Milling”, Annals of 15th COBEM, CDROM.

Araujo, A.C. & Silveira,J.L., 2001,“The influence of the specific cutting force on end milling models”, 16th COBEM.

Armarego, E. & Brown, J., 1969, “The Machining of Metals”, Prentice-Hall, New Jersey.

Ber, A., Rotberg, J. and Zombach, 1988, “A Method for Cutting Forces in End Milling”, Annals of CIRP, Vol. 37/1, pp. 37-40.

Jayaram, S., Kapoor, S. and DeVor, R., 2001, “Estimation of the Specific Cutting Pressures for Mechanistic Cutting Force Models”, Int. J. Mach. Tool. Man., Vol.41, pp. 265-281.

Kline, W., DeVor, R. and Lindberg, J., 1982, “The Prediction of Cutting Forces in End Milling”, Int. J. Mach. Tool. Des. Res., Vol.22/1, pp. 7-22.

Moufki, A., Dudzinski, D., Molinari, A. and Rausch, M., 2000, “Thermoviscoplastic modelling of oblique cutting: forces and chip flow predictions”, Int. J. Mech. Sci., Vol.42, pp. 1205-1232.

Tlusty, J. & MacNeil, P., 1975, “Dynamics of Cutting in End Milling”, Annals of the CIRP, Vol.24/1, pp. 213-221.

Yun, W.S. & Cho, D.W., 2001,“Accurate 3-D cutting force prediction using cutting condition independent coefficients in end milling”, Int. J. Mach. Tool. Man., Vol.41, pp. 463-478.

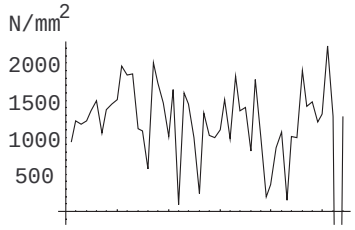

(a) K_{ct}

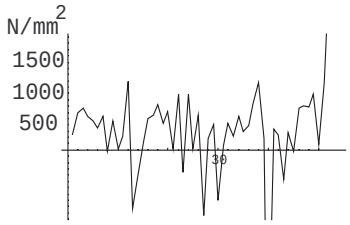

(b) K_{cr}

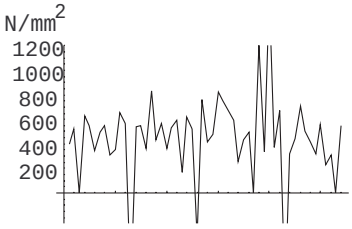

(c) K_{cz}

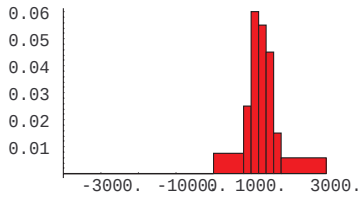

(d) K_{ct} Distribution

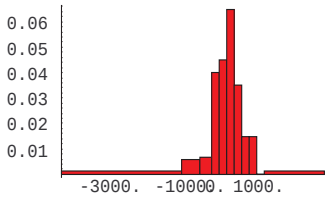

(e) K_{cr} Distribution

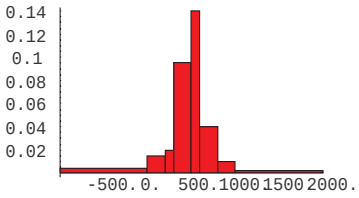

(f) K_{cz} Distribution

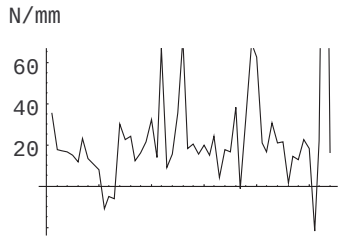

(g) K_{et}

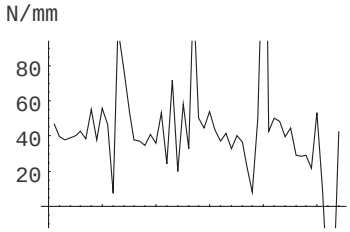

(h) K_{ec}

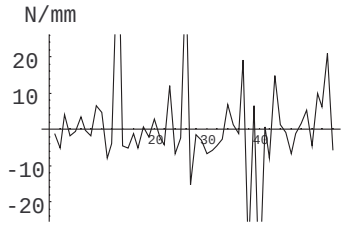

(i) K_{ez}

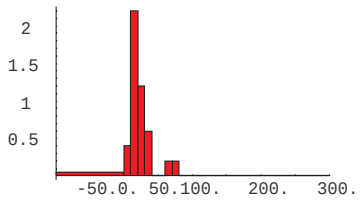

(j) K_{et} Distribution

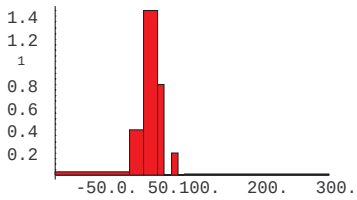

(k) K_{er} Distribution

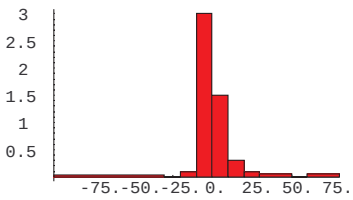

(l) K_{ez} Distribution

Figure 9: Experimental Specific Pressures and distribution

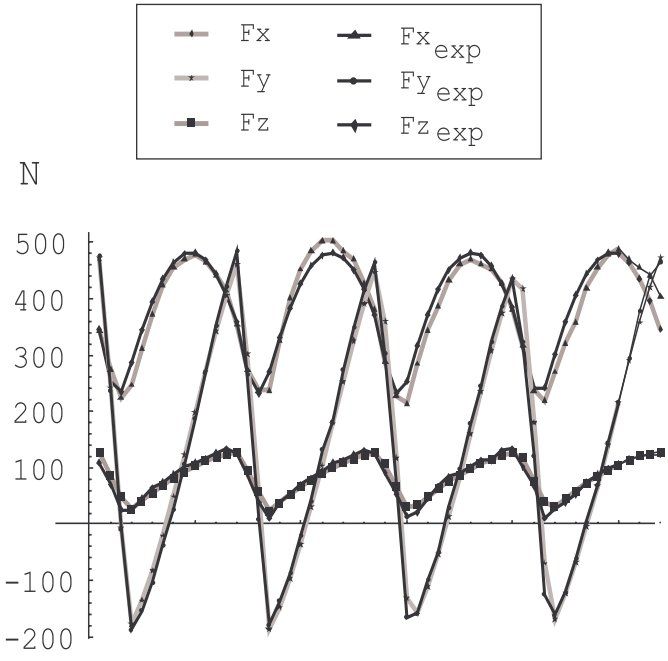

Figure 10: Comparison between experimental and theoretic forces